

## Gas Doping on the Topological Insulator $\text{Bi}_2\text{Se}_3$ Surface

Mohammad Koleini,<sup>1,2,\*</sup> Thomas Frauenheim,<sup>1</sup> and Binghai Yan<sup>1,†</sup>

<sup>1</sup>*Bremen Center for Computational Materials Science, University of Bremen, 28359 Bremen, Germany*

<sup>2</sup>*Hybrid Materials Interfaces Group, Faculty of Production Engineering, University of Bremen, 28359 Bremen, Germany*

(Received 15 June 2012; revised manuscript received 21 October 2012; published 2 January 2013)

Gas molecule doping on the topological insulator  $\text{Bi}_2\text{Se}_3$  surface with existing Se vacancies is investigated using first-principles calculations. Consistent with experiments,  $\text{NO}_2$  and  $\text{O}_2$  are found to occupy the Se vacancy sites, remove vacancy-doped electrons, and restore the band structure of a perfect surface. In contrast,  $\text{NO}$  and  $\text{H}_2$  do not favor passivation of such vacancies. Interestingly we have revealed a  $\text{NO}_2$  dissociation process that can well explain the speculative introduced “photon-doping” effect reported by recent experiments. Experimental strategies to validate this mechanism are presented. The choice and the effect of different passivators are discussed. This step paves the way for the usage of such materials in device applications utilizing robust topological surface states.

DOI: [10.1103/PhysRevLett.110.016403](https://doi.org/10.1103/PhysRevLett.110.016403)

PACS numbers: 71.20.Nr, 73.20.-r

Three-dimensional (3D) topological insulators (TI) have attracted extensive research interest recently [1–4]. Their novel topological surface states (TSS) in the bulk energy gap have great practical potential in spintronics and quantum computation by realizing the Majorana fermions [5]. However, most TI materials available today are poor insulators in the bulk due to heavy defect doping [[3,4,6] and references therein], hindering the utilization of the TSS in practice. To remove the bulk carriers, surface doping with gas molecules was adopted as a powerful tool in experiments [7–11], though the underlying detailed atomistic mechanisms are still unknown. Exploring chemical reactions and understanding the modified surface structures are crucial to comprehend the current experimental results and to help find new methods to achieve the bulk insulating state.

As of today, the most attractive TI material is  $\text{Bi}_2\text{Se}_3$  [7,12,13], demonstrating simple Dirac-type TSS along with a large bulk energy gap. Presumably due to the Se vacancies, however, it is found to be an  $n$ -doped semiconductor. To achieve a real bulk insulator,  $\text{NO}_2$  [7,9,11] and  $\text{O}_2$  [8,10] gas species were used to dope the surface and successively remove the donated bulk conduction electrons. In particular, the  $\text{NO}_2$  doped  $\text{Bi}_2\text{Se}_3$  surface exhibits a mysterious behavior, in which the surface loses electrons when exposed to photon flux in angle-resolved photoemission spectroscopy (ARPES) experiments [7,9]. This is very different from the cases of graphene [14] and another known TI material  $\text{Bi}_2\text{Te}_3$  [9,15], where the surface gains electrons back through desorbing  $\text{NO}_2$  stimulation or the so-called “photon-doping” method was employed to manipulate the surface bands in experiments [15], the underlying mechanism remains to be defined. In this Letter, we study from first principles the reaction of gas molecules on the  $\text{Bi}_2\text{Se}_3$  surface containing Se vacancies and conclude how these affect the TSS.

First-principles molecular dynamics (FPMD) simulations were employed to investigate the dynamic process

of chemical adsorption and search for the stable atomic configurations. In bulk  $\text{Bi}_2\text{Se}_3$ , five atomic layers form a quintuple layer (QL) while the coupling between two such QLs is of the van der Waals type [12]. We used a slab model to simulate the surface and the slab contains  $3 \times 3$  primitive unit cells in the  $xy$  plane. In the MD simulation a vacancy and the adsorbed molecule were placed only on the top surface of the slab. We have tested that a 2-QL slab is thick enough for MD, as calculations with a thicker slabs (e.g. 3 QLs) produced the same molecular trajectories. FPMD calculations including van der Waals interactions [16] have been performed at 300 K in the microcanonical ensemble with an integration time step of 1.0 fs [17]. We let the calculation run for 5.0 ps, while in the worst case, roughly after 1.5 ps, no more significant structural changes were observed. In the electronic structure calculations we used a 7-QL slab, where the MD optimized 2 QLs constitute the outermost layers of the top and bottom surfaces and the middle 3 QLs were obtained from the bulk structure. The adsorbates and the vacancy have been placed on both surfaces to impose the inversion symmetry. These structures are depicted in the Supplemental Material [18]. The thickness of 7 QLs prevents the interaction between the top and bottom surface states [19,20]. Subsequently, band structure and density of states calculations were carried out to investigate the electronic properties [18].

The results are shown in Fig. 1. The pristine surface has a single pair of Dirac-like TSS with the Fermi level  $E_F$  crossing the Dirac point at  $\bar{\Gamma}$ , consistent with previous calculations [12]. When a Se vacancy forms on the surface,  $E_F$  shifts to the bulk conduction band bottom, resulting in  $n$ -type doping as observed in experiments. Interestingly, the surface states are energetically changed considerably by the existing vacancies. The original Dirac point at  $\bar{\Gamma}$  shifts upward and almost merges into the conduction band, while a new Dirac point forms at the  $\bar{M}$  point [Fig. 1(b)]. In the bulk gap,  $E_F$  still intersects the TSS odd times,

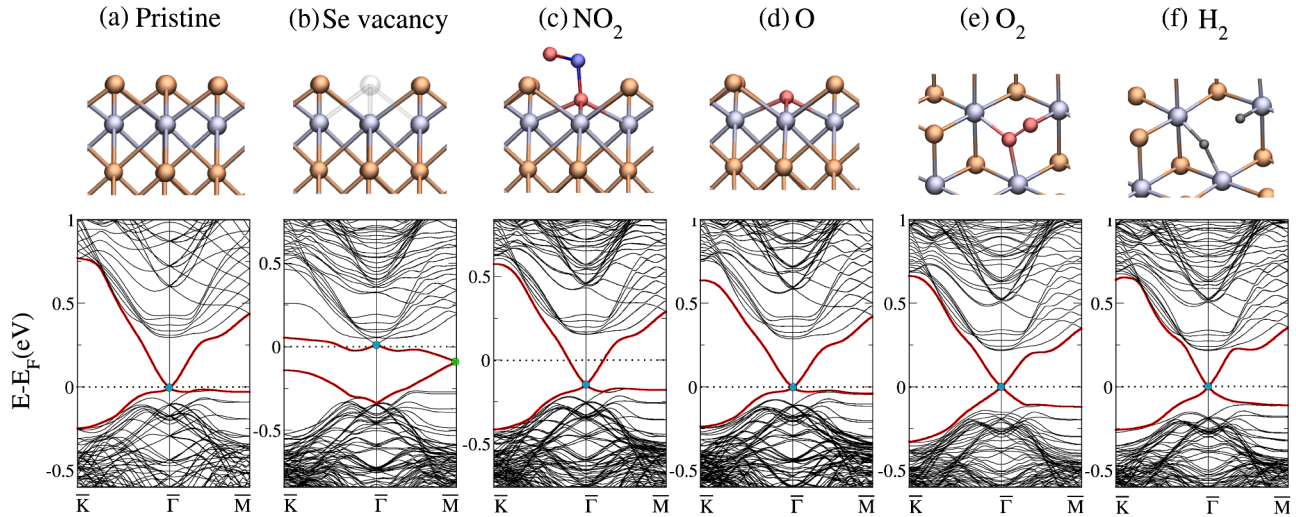


FIG. 1 (color online). Atomic structures and band structures for (a) a perfect  $\text{Bi}_2\text{Se}_3$  surface, (b) a surface with a Se vacancy, (c)  $\text{NO}_2$  adsorption, (d) O adsorption from the dissociated  $\text{NO}_2$ , (e)  $\text{O}_2$  adsorption, and (f)  $\text{H}_2$  adsorption. Bands are aligned to their valence band maximum at  $\bar{\Gamma}$ . The Fermi energy is shifted to zero. (a)–(d) show structures from the side view, whereas (e),(f) show structures from the top view. Red (thick) lines indicate the surface states. The transparent ball indicates the missing Se at the vacancy in (b). Band structures are calculated from a  $3 \times 3$  supercell of 7 QLs thick. Colored circles denote Dirac points.

indicating the topological nontrivial character. It should be noted that in our model Se vacancies distribute periodically on the surface, reflecting the employed supercell periodic boundary condition. However due to the vacancy random distribution on the real sample surfaces, ARPES measured only a single Dirac point at  $\bar{\Gamma}$  in the primitive Brillouin zone [7,13,21]. This illustrates a possible way to engineer the Dirac point by designing a well-ordered surface potential.

$\text{NO}_2$  and NO.—In the FPMD simulations,  $\text{NO}_2$  molecules are placed above both the pristine surface and the surface with a vacancy. On the pristine surface, most simulations show that  $\text{NO}_2$  moves freely above the surface and does not adsorb, while rare simulations reveal that  $\text{NO}_2$  attaches to the surface without bouncing back to the gas phase, having an adsorption potential energy (APE) of 0.3 eV. However, on the defected surface  $\text{NO}_2$  chemisorbed at the vacancy site quickly. One of the  $\text{NO}_2$  oxygens, denoted as O1, adsorbs and binds to three Bi atoms from the second atomic layer [see Fig. 2(a), step II]. At the beginning of the formation of Bi-O1 bonds,  $\text{NO}_2$  and its neighboring surface atoms locally have very high momenta due to the instantaneous adsorption, initializing a state out of thermodynamic equilibrium. Proceeding further, different FPMD replicas resulted into two situations. We have performed totally thirty MD simulations. In most of the simulations,  $\text{NO}_2$  eventually adsorbs stably on the surface. The molecule exhibits an APE of  $-2.0$  eV. The equilibrium bond length of N-O1 is elongated to 1.6 Å compared to the second N-O bond of 1.3 Å, indicating a weakened N-O1 bond upon adsorption. The corresponding band structure is depicted in Fig. 1(c), whereby the Dirac

cone is recovered at  $\bar{\Gamma}$ . However, the surface is yet slightly electron doped with  $E_F$  0.15 eV above the Dirac point. This indicates that  $\text{NO}_2$  cannot take away all donor electrons from the vacancy. On the other hand, in two MD simulations  $\text{NO}_2$  starts dissociating via breaking the weak N-O1 bond at a time of about 1 ps after the adsorption. Subsequently,  $\text{NO}_2$  dissociates into NO that leaves the surface and an O1 atom that passivates the vacancy. To estimate the dissociation energy barrier, we performed density-functional calculations using the nudged elastic band (NEB) method [22] and monitor that dissociation happens smoothly with a barrier of about 0.4 eV [spin-orbit coupling (SOC) is found to increase this value by 0.3 eV]. As mentioned above, the  $\text{NO}_2$  adsorption induces an initial state out of equilibrium, which can be understood as a “hot precursor” [23]. As a hot precursor, the adsorbed  $\text{NO}_2$  exhibits higher energy and a substantially greater probability of relevant reactions (e.g., dissociation) than the probability for the same molecule within thermal equilibrium on the surface. By analyzing the atom trajectories,  $\text{NO}_2$  is found to pass through a barrier of about 0.1 eV during dissociation. One can find that this MD barrier is much smaller than the NEB result, which can be treated as a barrier for an equilibrated system. In addition, we have also performed MDs using the molecularly adsorbed  $\text{NO}_2$  as the initial state. In this case, the energy of a hot precursor is fully dissipated in advance and therefore dissociation does not happen. In real experiments, the adsorbed  $\text{NO}_2$  molecules may quickly reach stable configurations with dissipating additional energies and adsorb on the surface. If the system is driven out of thermodynamic equilibrium due to a strong excitation, the adsorbed  $\text{NO}_2$  can possibly

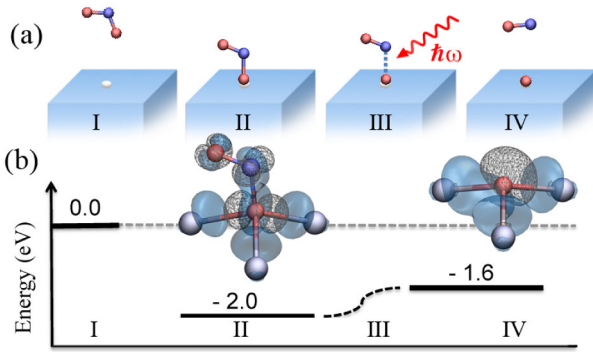


FIG. 2 (color online). (a) Schematic of NO<sub>2</sub> molecule adsorption and dissociation processes and (b) corresponding reaction energetics on the Bi<sub>2</sub>Se<sub>3</sub> surface with a Se vacancy. (SOC is not included in these energies) The Se vacancy is indicated by the white dot (step I) and donates two electrons that can dope the surface. During NO<sub>2</sub> exposure, the molecule occupies the vacancy site quickly with one O binding to three Bi atoms from the second atomic layer (step II). The corresponding N-O bond becomes weaker compared to before adsorption (step I). The stable adsorption structure is shown in (b) together with the charge density difference before and after adsorption. The donor electrons transfer partially from the vacancy to NO<sub>2</sub>. Under external photon exposure (step III), the weakened N-O bond breaks, resulting in NO<sub>2</sub> dissociation into NO + O (step IV). The NO molecule leaves the surface, while O passivates the vacancy. In this case, two donor electrons transfer to the O atom and the vacancy is compensated. White balls stand for Bi atoms, red for O, and blue for N. In the isovalue surface plots of the charge difference, solid blue (wired gray) color denotes charge depletion (gain).

dissociate. From the related band structure in Fig. 1(d), we see the O1 atom passivation shifts  $E_F$  further down to the Dirac point and totally restores the band structure of the pristine surface. This can be understood by the fact that the single O1 atom can accommodate all two extra electrons from the Se vacancy, more than NO<sub>2</sub> in the former case, as illustrated by the charge density change in Fig. 2(b). Contrary to NO<sub>2</sub>, NO binds weakly (APE of  $-0.6$  eV) and does not yield a good passivation of the vacancy, due to its much lower electron affinity.

It is interesting to compare these results with recent ARPES measurements [7,15]. In experiments, the Fermi level is  $0.3$  eV above the Dirac point. Supposing all doped electrons are due to the Se vacancies, a dosage of  $0.1$  Langmuir (L) of NO<sub>2</sub> can shift  $E_F$  down by  $0.15$  eV. After dosing with NO<sub>2</sub>, in experiment two additional non-dispersive peaks appear at the binding energies of  $-4.0$  eV and  $-7.5$  eV [7]. This agrees with our calculated density of states (DOS) projected onto NO<sub>2</sub> [Fig. 3(b)], where partial DOS analysis (not shown here) indicates that the peak at  $\sim -4.0$  eV is mainly due to both O atoms and the other at  $\sim -7.5$  eV is due to all N and O atoms. The ARPES results are found to remain stable with temperature varying from  $10$  to  $300$  K. As discussed above, both the

APE on the pristine surface and the dissociation barrier (NEB barrier) are higher than the room temperature thermal fluctuations. Therefore, NO<sub>2</sub> will not desorb or dissociate at  $300$  K, consistent with the experiment. Moreover, the surface with a dose of  $0.1$  L can also be further hole doped by extensive photon (energy  $28$ – $55$  eV) exposure until  $E_F$  reaches the Dirac point [15], called “photon doping.”

Considering that NO<sub>2</sub> molecules can possibly dissociate into NO + O under laser pulse irradiation [24], the above experimental observation may be explained by the NO<sub>2</sub> dissociation process (Fig. 2, step III). As aforementioned, the N-O1 bond turns weaker after NO<sub>2</sub> adsorption. Thus, photons can excite the adsorbed NO<sub>2</sub> and the surface atoms, and eventually stimulate the N-O1 bond to break. Consequently, the dissociation leaves on the O1 atom in the vacancy, resulting in extra charge transfer from the vacancy to the O1 atom. Finally  $E_F$  is shifted down to the Dirac point. Therefore, we conclude that a dosage of  $0.1$  L of NO<sub>2</sub> passivates most of the Se vacancies on the surface, as the experimental  $E_F$  position ( $0.15$  eV above the Dirac point) is the same as our calculated one [see Fig. 1(c)]. Subsequently, photon exposure induces an O-passivated surface without extra donor electrons. In addition, without photon exposure a dosage of  $2.0$  L more can also shift  $E_F$  down to the Dirac point [7,15]. This can be attributed to the weak adsorption of NO<sub>2</sub> on the pristine surface (see above) where much less electron transfer happens compared to that of the strong adsorption on the vacancy.

The proposed dissociation mechanism can be easily checked in experiments. One way is to monitor whether the composition of NO (NO<sub>2</sub>) increases (decreases) after photon exposure. The second way is to measure the valence band spectra. We predicted that the peak at  $\sim -7.5$  eV will become weaker or even disappear after extensive photon exposure, as indicated by the projected DOS in Fig. 3(c). The third alternative is to observe the surface using STM or from vibration spectra. Additionally, one can find that monoatomic oxygen can be an excellent passivator to Se vacancies if under controllable exposure.

O<sub>2</sub> and H<sub>2</sub>.—The O<sub>2</sub> molecule also gets adsorbed in the vacancy site quickly with an estimated APE of  $-3.4$  eV. The two O atoms still remain connected to each other with one O (labeled as O1) binding to one Bi atom and the other O (O2) binding to the other two Bi atoms, as Fig. 1(e) shows. In the equilibrium structure, the O1-Bi bond length is  $\sim 2.2$  Å, while two O2-Bi bonds form at  $\sim 2.4$  Å. The O<sub>2</sub> bond is stretched to  $1.4$  Å from the equilibrium distance of  $1.2$  Å. Concluding from the band structure analysis, O2 captures two extra electrons from the vacancy and recovers the neutral-charged TSS very well. After adsorption no O<sub>2</sub> dissociation was observed in any of our MD simulations, clearly due to the stiffness of the O = O bond. This suggests why photon exposure had no improving effect in experiments with O<sub>2</sub> [8,10]. It is known that O<sub>2</sub> can

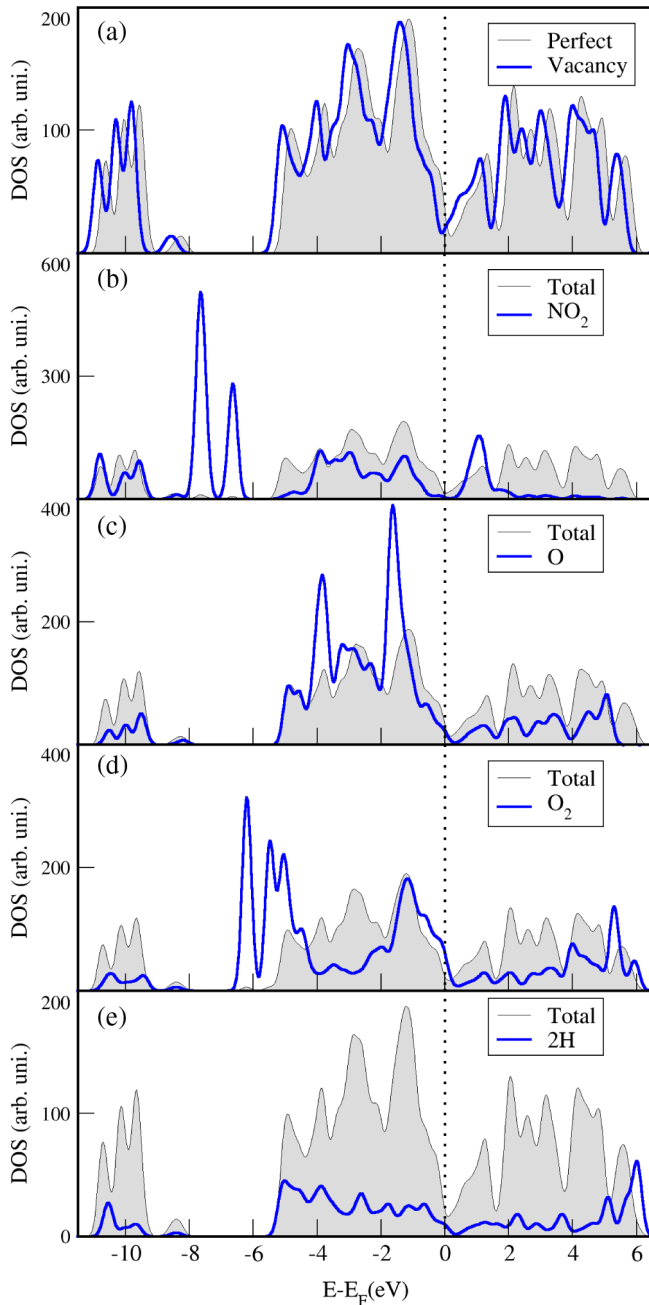


FIG. 3 (color online). Density of states (DOS) for (a) the perfect pristine surface and the one with a Se vacancy, (b)  $\text{NO}_2$ , (c) a single O atom, (d)  $\text{O}_2$ , and (e)  $\text{H}_2$  passivated. To be more clear, the adsorbate's partial DOS has been scaled by  $N_X/N_{\text{Tot}}$ , where  $N_X$  is the number of atoms in the adsorbate and  $N_{\text{Tot}}$  is the total number of atoms in the supercell.

dissociate on some metal surfaces [25–32], called a “Coulomb explosion.” Therein electrons tunnel through the metal valence band to the affinity level of  $\text{O}_2$  non-adiabatically. The excess electrons occupy the antibonding molecule orbital and lead to rapid dissociation of  $\text{O}_2$ . However, we did not observe the  $\text{O}_2$  dissociation in current calculations. For Coulomb repulsion, the work function of the metal surface is known to play an important role, where

a low work function can induce a nonadiabatic charge transfer process [33]. Here, the  $\text{Bi}_2\text{Se}_3$  surface is found to have a much larger work function of about 5.7 eV [calculated by density-functional theory (DFT)] than normal metals (such as Al and Cs). Consequently, electrons can hardly tunnel from  $\text{Bi}_2\text{Se}_3$  to the  $\text{O}_2$  molecule in a ballistic course. This may explain why  $\text{O}_2$  dissociation does not occur in our case. On the other hand,  $\text{H}_2$  does not occupy the vacancy site in the MD adsorption simulations. However, after artificially saturating dangling bonds with hydrogens, the relaxed structure shows similar bondings with three underlying Bi atoms as in the  $\text{O}_2$  case [see Fig. 1(f)]. This passivation can also restore a perfect Dirac-type band structure [see Fig. 1(f)]. Though  $\text{H}_2$  adsorption and dissociation is not favored in dynamics, single H atoms can be an ideal passivation to Bi dangling bonds in theoretical studies, removing trivial surface dangling bond states and simplifying the underlying physics.

In summary, we have studied the chemical adsorption of gas molecules ( $\text{NO}_2$ ,  $\text{NO}$ ,  $\text{O}_2$ , and  $\text{H}_2$ ) on the  $\text{Bi}_2\text{Se}_3$  surface. The passivation of common Se surface vacancies is found to gain donor electrons much more effectively than weak adsorption on the pristine surface. The local atomic structures after adsorption are revealed and the band structures are compared. For example,  $\text{NO}_2$  can exhibit two kinds of adsorption on the surface with vacancy defects: adsorption on Se vacancies and adsorption on the pristine surface. In general, the vacancy adsorption is more favorable than the latter due to the strong chemical binding if vacancies exist.  $\text{NO}_2$  is observed to passivate the vacancy and accommodate partially the vacancy-doped electrons. By overcoming a considerable energy barrier (e.g., with laser stimulation),  $\text{NO}_2$  dissociates into  $\text{NO}$  and a single O atom, whereby the latter occupies the vacancy and accommodates all donor electrons. This dissociation and charge transfer can explain the mysterious “photon-doping” effect seen in ARPES experiments. Moreover, both  $\text{O}_2$  molecules and single O atoms are found to passivate the vacancy very well and restore the surface band structure to the charge neutral state. In contrast,  $\text{NO}$  and  $\text{H}_2$  are not favorable adsorbates on the  $\text{Bi}_2\text{Se}_3$  surface. It is worth mentioning that a  $\text{Bi}_2\text{Te}_3$  sample contains rarely Te vacancies and  $\text{NO}_2$  has only physical adsorption on the surface (the adsorption energy is 0.4 eV in our DFT calculation). As mentioned before, photon exposure will remove the physically adsorbed  $\text{NO}_2$  on  $\text{Bi}_2\text{Te}_3$  surface and terminate the gas doping effect [9,15]. The combination of MD with electronic structure analysis is shown to be versatile in explaining experimental observations along with suggesting new routes for device engineering, by tailoring different dopants and TI materials.

We acknowledge Professor Y. L. Chen at the University of Oxford, Dr. J. M. Knaup at the University of Bremen, and Dr. I. Kiss at the Max-Planck Institute for Chemical Physics of Solids for fruitful discussions. M. K.

acknowledges financial support from state of Bremen. B. Y. acknowledges financial support from the Alexander von Humboldt Foundation in Germany. Computation time has been allocated at the University of Bremen and the Supercomputer Center of Northern Germany (HLRN).

\*koleini.m@gmail.com

†bhyan@bccms.uni-bremen.de

- [1] X.-L. Qi and S.-C. Zhang, *Phys. Today* **63**, No. 1, 33 (2010).
- [2] J. Moore, *Nature (London)* **464**, 194 (2010).
- [3] M. Z. Hasan and C. L. Kane, *Rev. Mod. Phys.* **82**, 3045 (2010).
- [4] X.-L. Qi and S.-C. Zhang, *Rev. Mod. Phys.* **83**, 1057 (2011).
- [5] L. Fu and C. L. Kane, *Phys. Rev. Lett.* **100**, 096407 (2008).
- [6] B. Yan and S.-C. Zhang, *Rep. Prog. Phys.* **75**, 096501 (2012).
- [7] D. Hsieh, Y. Xia, D. Qian, L. Wray, J. Dil, F. Meier, J. Osterwalder, L. Patthey, J. Checkelsky, N. Ong *et al.*, *Nature (London)* **460**, 1101 (2009).
- [8] Y. Chen, J. Chu, J. Analytis, Z. Liu, K. Igarashi, H. Kuo, X. Qi, S. Mo, R. Moore, D. Lu *et al.*, *Science* **329**, 659 (2010).
- [9] Y. Xia, D. Qian, D. Hsieh, R. Shankar, H. Lin, A. Bansil, A. Fedorov, D. Grauer, Y. Hor, R. Cava *et al.*, [arXiv:0907.3089](https://arxiv.org/abs/0907.3089).
- [10] D. Hsieh, J. W. McIver, D. H. Torchinsky, D. R. Gardner, Y. S. Lee, and N. Gedik, *Phys. Rev. Lett.* **106**, 057401 (2011).
- [11] L. Wray, S. Xu, M. Neupane, Y. Xia, D. Hsieh, D. Qian, A. Fedorov, H. Lin, S. Basak, Y. Hor *et al.*, [arXiv:1105.4794](https://arxiv.org/abs/1105.4794).
- [12] H. Zhang, C.-X. Liu, X.-L. Qi, X. Dai, Z. Fang, and S.-C. Zhang, *Nat. Phys.* **5**, 438 (2009).
- [13] Y. Xia, D. Qian, D. Hsieh, L. Wray, A. Pal, H. Lin, A. Bansil, D. Grauer, Y. S. Hor, R. J. Cava *et al.*, *Nat. Phys.* **5**, 398 (2009).
- [14] S. Y. Zhou, D. A. Siegel, A. V. Fedorov, and A. Lanzara, *Phys. Rev. Lett.* **101**, 086402 (2008).
- [15] Y. Xia, Ph.D. thesis, Princeton University, 2010.
- [16] S. Grimme, J. Antony, S. Ehrlich, and H. Krieg, *J. Chem. Phys.* **132**, 154104 (2010).
- [17] In the system containing hydrogen the time step was decreased to 0.2 fs to cope with high frequency oscillations of H atoms.
- [18] See Supplemental Material at <http://link.aps.org/supplemental/10.1103/PhysRevLett.110.016403> for simulation details.
- [19] C.-X. Liu, H. J. Zhang, B. Yan, X.-L. Qi, T. Frauenheim, X. Dai, Z. Fang, and S.-C. Zhang, *Phys. Rev. B* **81**, 041307 (2010).
- [20] H.-Z. Lu, W.-Y. Shan, W. Yao, Q. Niu, and S.-Q. Shen, *Phys. Rev. B* **81**, 115407 (2010).
- [21] Y. L. Chen, J. G. Analytis, J.-H. Chu, Z. K. Liu, S.-K. Mo, X. L. Qi, H. J. Zhang, D. H. Lu, X. Dai, Z. Fang *et al.*, *Science* **325**, 178 (2009).
- [22] G. Henkelman, B. Uberuaga, and H. Jónsson, *J. Chem. Phys.* **113**, 9901 (2000).
- [23] J. Harris and B. Kasemo, *Surf. Sci.* **105**, L281 (1981).
- [24] G. E. Busch and K. R. Wilson, *J. Chem. Phys.* **56**, 3626 (1972); **56**, 3638 (1972).
- [25] B. Kasemo, *Phys. Rev. Lett.* **32**, 1114 (1974).
- [26] B. Kasemo, E. Törnqvist, J. Nørskov, and B. Lundqvist, *Surf. Sci.* **89**, 554 (1979).
- [27] J. Nørskov, D. Newns, and B. Lundqvist, *Surf. Sci.* **80**, 179 (1979).
- [28] A. Böttcher, R. Imbeck, A. Morgante, and G. Ertl, *Phys. Rev. Lett.* **65**, 2035 (1990).
- [29] H. Brune, J. Wintterlin, R. J. Behm, and G. Ertl, *Phys. Rev. Lett.* **68**, 624 (1992).
- [30] T. Greber, *Chem. Phys. Lett.* **222**, 292 (1994).
- [31] L. Hellberg, J. Strömquist, B. Kasemo, and B. I. Lundqvist, *Phys. Rev. Lett.* **74**, 4742 (1995).
- [32] A. J. Komrowski, J. Z. Sexton, A. C. Kummel, M. Binetti, O. Weiße, and E. Hasselbrink, *Phys. Rev. Lett.* **87**, 246103 (2001).
- [33] G. Katz, Y. Zeiri, and R. Kosloff, *Surf. Sci.* **425**, 1 (1999).